Applied Magnetic Resonance (2020) 51:523–543
https://doi.org/10.1007/s00723-020-01199-w

Applied
Magnetic Resonance

ORIGINAL PAPER

Potential of Isotope Substitution in EPR Studies of Nitroxide Biradicals

R. B. Zaripov[1] · I. T. Khairutdinov[1] · T. Kálai[2,3] · K. Kish[2] · A. I. Kokorin[4,5] · K. M. Salikhov[1]

Received: 23 December 2019 / Revised: 29 March 2020 / Published online: 30 April 2020

Abstract

New nitroxide biradicals $^{15}NR_6$–C≡C–$(p$-$C_6H_4)_2$–C≡C–$^{14}NR_6$ (**B2**) and $^{15}NR_6$–C≡C–$(p$-$C_6H_4)_2$–C≡C–$^{15}NR_6$ (**B3**), where R_6 denotes 1-oxyl-2,2,6,6-tetramethyl–1,2,3,6-tetrahydropyridine ring, are synthesized and studied in liquid solutions by continuous-wave electron paramagnetic resonance (EPR) spectroscopy. Hyperfine interaction constants and exchange integrals are determined from the simulation and fitting of experimental spectra and calculated ones. The best fitting of the EPR spectra detected in experiments and their temperature dependence was achieved under the assumption that the biradicals perform transitions between conformations with different exchange integrals. The conformation of about 75% of biradicals has the exchange integral $|J| = 4.4$ G. Thus, the ground electronic state of these biradicals has the conformation with $|J| = 4.4$ G. About 20% of biradicals have the conformation with the zero exchange integral. A minor fraction of biradicals have conformations with $|J| = 11.2$ G and $|J| = 57$ G. The activation energy for the transition from the conformation with $|J| = 4.4$ G to the conformation with $J = 0$ is 8.5 kcal/mol, while that for the reverse reaction is 1.7 kcal/mol. It is shown that the isotope substitution provides a valuable resource in the EPR studies of the exchange interaction in biradicals.

✉ R. B. Zaripov
zaripov.ruslan@gmail.com

[1] Zavoisky Physical-Technical Institute, FRC Kazan Scientific Center of RAS, Kazan, Russian Federation

[2] Inistitute of Organic and Medicinal Chemistry, University of Pécs, Pécs, Hungary

[3] Szentágothai Research Center, Pécs, Hungary

[4] N. N. Semenov Federal Research Center for Chemical Physics, Russian Academy of Sciences, Moscow, Russian Federation

[5] Plekhanov Russian University of Economics, Moscow, Russian Federation

1 Introduction

Electron paramagnetic resonance (EPR) studies of biradicals make it possible to obtain information on the exchange interaction between radical centers, which are connected by a system of covalent bonds, and the effect of the bond conjugation on the exchange interaction between two radical centers in biradicals. EPR data can also give unique information about transitions of biradicals between different conformations including the rate constants of these monomolecular reactions [1].

Numerous nitroxide biradicals with different compositions and structures are known nowadays ([1–7] and references therein). One may expect that conjugation of valence bonds in a "bridge" results in a rigid molecular structure. The rigid molecular structures may be of advantage for studying mechanisms of the exchange interaction, e.g., direct or indirect exchange or superexchange [8]. An important application of biradicals is their usage as polarization agents for dynamic nuclear polarization (DNP). Biradicals may be of importance for the optimization of the DNP enhancement [9, 10] and the implementation of two-qubit quantum logic operations [11].

A series of biradicals R_6–$(C{\equiv}C)_n$–R_6, where R_6 is 1-oxyl-2,2,6,6-tetramethyl-1,2,3,6-tetrahydropyridine ring, and $n = 0$–3 were studied taking these aspects into consideration [12–16]. They made it possible to study the dependence of the exchange integral on the length of the bridge between unpaired electrons in biradicals by varying the number of CC groups [17–19]. Biradicals R_6–C≡C–*p*-C_6H_4–C≡C–R_6 and R_5–C≡C-(*p*-C_6H_4)$_2$-C≡C–R_5 (R_5 is 1-oxyl-2,2,5,5-tetramethyl-pyrroline-group) were also studied by EPR spectroscopy [15, 20–22].

The biradicals R_6–$(C{\equiv}C)_n$–R_6 with $n = 1$, 2 were expected to be rigid because of the conjugation of double bonds in the nitroxide rings with triple bonds of the acetylene bridge. However, the UDFT/B3LYP/cc-pVDZ calculations have shown [20] that the barriers for the intramolecular rotation around single bonds in the bridge do not exceed 1 and 8 kJ/mol for biradicals R_6–C≡C–C≡C–R_6 and R_6–C≡C–*p*-C_6H_4–C≡C–R_6, respectively. Hence, this intramolecular rotation can proceed rather fast at room temperatures. EPR spectra and the results of DFT calculations of several biradicals such as R_6–^{13}C≡C-*p*-C_6H_4–C≡^{13}C–R_6 and R_5–C≡^{13}C–(*p*-C_6H_4)$_2$–^{13}C≡C–R_5 upon the isotope substitution have been studied in [23, 24].

It is well-known [1] that manifestations of the exchange interaction between two radical centers in biradicals depend on the splitting of EPR lines induced by the hyperfine interaction (HFI) of unpaired electrons with magnetic nuclei. That is why the isotope substitution in biradicals is of particular interest for studying spin–spin interactions using the EPR technique. Indeed, within the Born–Oppenheimer approximation, the isotope substitution in biradicals does not change their structure, spin density distribution of unpaired electrons, electron spin-dependent exchange, and dipole–dipole interactions. The isotope substitution changes the value of the nucleus spin and the HFI constant a of the unpaired electron since different isotopes have different gyromagnetic ratios for their nuclear spins. Thus, the ratio between the exchange integral J and the HFI constant a of the resonance

frequencies also changes at the isotope substitution. The manifestation of the exchange interaction in the EPR spectrum depends on this ratio. Therefore, the isotope substitution provides an additional resource for determining the exchange integral using EPR spectroscopy data. In this work, we used the potential advantages of the isotope substitution when studying the exchange interaction in nitroxide biradicals.

Magnetically symmetric biradicals $^{14}NR_6$–C≡C–(p-C_6H_4)$_2$–C≡C–$^{14}NR_6$ (**B1**) were studied in [22]. Symmetric biradicals have an interesting feature: their EPR spectrum does not manifest any effect of the scalar Heisenberg exchange interaction under certain conditions. This occurs when unpaired electrons of two radical centers have the same local magnetic fields, so that they become magnetically equivalent. As a result, it is a problem to find a fraction of biradicals with the zero exchange integral. We discuss this problem in detail below in Sect. 3. One way to solve this problem is to use asymmetric nitroxide biradicals.

In this study, we report our experimental and theoretical results on the features of EPR spectra for two new synthesized nitroxide biradicals $^{15}NR_6$–C≡C–(p-C_6H_4)$_2$–C≡C–$^{14}NR_6$ (magnetically asymmetric biradical **B2**) and $^{15}NR_6$–C≡C–(p-C_6H_4)$_2$–C≡C–$^{15}NR_6$ (magnetically symmetric **B3**).

This work illustrates that the isotope substitution is a useful approach to studying the exchange interaction in biradicals using EPR spectroscopy.

2 Experiment

2.1 Synthesis of Biradicals

New $^{15}N/^{14}N$ and $^{15}N/^{15}N$ biradicals **B2** and **B3** were synthesized from compounds **1** [25] and **4** [26] prepared according to the published procedures. The synthesis procedure for **B2** and **B3** is shown in Fig. 1 and described below in detail. Compound **1** was synthesized from $^{15}NH_4Cl$ (95% VEB-Berlin-Chemie) as described in [21] but without deuteration. 4,4′-Diethinylbiphenyl was purchased from TCI (Tokyo Chemical Industry), other reagents were purchased from Aldrich or Alfa Aesar. Anhydrous tetrahydrofurane (THF) was used and Et_3N was distilled from CaH_2 prior to use. Melting points were determined with a Boetius micro melting point apparatus and are uncorrected. Elemental analyses (C, H, N, S) were performed on a Fisons EA 1110 CHNS elemental analyzer. Mass spectra were recorded on a Thermoquest Automass Multi. IR spectra were taken on a Bruker Alpha FT-IR instrument with ATR support (ZnSe plate). Flash column chromatography was performed on Merck Kieselgel 60 (0.040–0.063 mm). Qualitative thin-layer chromatography (TLC) was carried out on commercially available plates (20×20×0.02 cm) coated with Merck Kieselgel GF254.

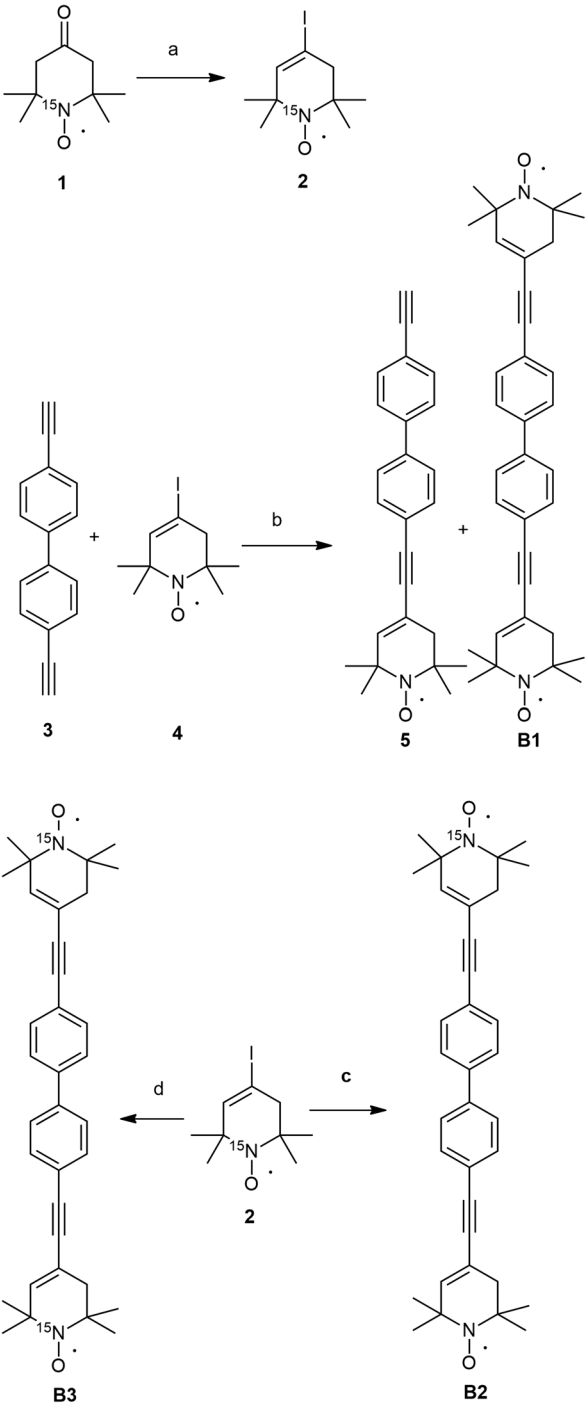

Fig. 1 Scheme of synthesis of $^{15}N/^{14}N$ and $^{15}N/^{15}N$ biradicals

2.2 4-Iodo-2,2,6,6-tetramethyl-5,6-dihydropyridin-(1-^{15}N)-1(2H)-yloxyl Radical (2)

Compound **1** (1.71 g, 10.0 mmol) dissolved in EtOH (10 mL) was added dropwise to hydrazine hydrate (0.06 mol, 3.0 mL) during 3 h, then the mixture was boiled at gentle reflux for 1 h. After cooling, the colorless solution was evaporated to dryness, the residue was taken up in a mixture of $CHCl_3$–MeOH (9:1, 15 mL). The organic phase was washed with brine (5 mL), separated, the organic phase dried ($MgSO_4$) with addition of PbO_2 (239 mg, 1.0 mmol). After bubbling with O_2 for 30 min, the mixture was filtered, evaporated, and the residue (crude hydrazone) was used immediately in the next step. The crude hydrazone was dissolved in anhydr. THF (10 mL) and added dropwise to a stirred solution of I_2 (5.08 g, 20.0 mmol) and tetramethylguanidine (4.025 g, 35.0 mmol) in THF (10 mL). After addition of hydrazine, the mixture was stirred at r. t. for 2 h, diluted with Et_2O (30 mL), water (20 mL), and 5% aq. H_2SO_4 (15 mL). The organic phase was dried ($MgSO_4$), filtered, and evaporated. The crude product was subjected to flash column chromatography (hexane-Et_2O). The first green band was discarded and the second pink-orange band contained compound **2**. Deep orange solid 860 mg (30%), melting point (mp) 63–65 °C, R_f: 0.70 (hexane-Et_2O), 2:1. IR: 1649 cm^{-1} (C=C), MS (EI): *m/z* (%) = 281 (M^+, 22), 249(6), 154 (37), 139 (69), 81 (100). Anal. Calcd. for $C_9H_{15}I^{15}NO$: C, 38.45; H, 5.38; N, 5.34. Found: C, 38.55; H, 5.37; N, 5.30.

4-((4′-ethynyl-[1,1′-biphenyl]-4-yl)ethynyl)-2,2,6,6-tetramethyl-5,6-dihydropyridin-1(2*H*)-yloxyl radical (**5**) and 4,4′-([1,10-Biphenyl]-4,4′-diylbis(ethyn-2,1-diyl)) bis(2,2,6,6-tetramethyl-5,6-dihydropyridin-1(2*H*)-yloxyl) biradical (**B1**). To a degassed solution of **3** (606 mg, 3.0 mmol) in THF (50 mL), Et_3N (2.0 mL), CuI (10 mg, 0.05 mmol), and Pd (PPh_3)$_4$ (25 mg, 0.02 mmol) were added under N_2 and compound **4** (280 mg, 1.0 mmol) in THF (10 mL) was added dropwise. After stirring the mixture 3 h at room temperature, it was filtered through Celite, the solvent was evaporated and the residue was dissolved in CH_2Cl_2 (15 mL), washed with brine (10 mL), the organic phase was separated, dried ($MgSO_4$), activated MnO_2 (86 mg, 1.0 mmol) were added, and O_2 was bubbled for 15 min. The mixture was set aside for 6 h, then filtered, evaporated, and the residue was purified by flash column chromatography (hexane/Et_2O) to yield compound **5** at R_f = 0.51 (hexane-Et_2O/2:1), as a yellow solid 120 mg (33%), mp 172–173 °C, IR: 3219 (≡CH), 2101 (C≡C), 1684, 1602 (C=C), MS (EI): *m/z* (%) = 354 (M^+, 16), 340 (33), 324 (76), 309 (36), 281 (51), 42 (100). Anal. Calcd. for $C_{25}H_{24}NO$: C, 84.71; H, 6.82; N, 3.95; O, 4.51. Found: C, 84.60; H, 6.77; N, 4.01. The second compound at R_f: 0.25 (hexane/Et_2O, 2:1) was biradical **B1** [22] 80 mg (31%), deep yellow solid, mp 230–232 °C. IR = 1650 cm^{-1} (C=C), MS (EI): *m/z* (%) = 506 (M^+, 32), 491(45), 476 (56), 461 (85), 446 (75), 165 (100). Anal. Calcd. for $C_{34}H_{38}N_2O_2$ C, 80.60; H, 7.56; N, 5.53. Found: C, 80.56; H, 7.45; N, 5.49.

2.3 4,4′-([1,10 -Biphenyl]-4,4′ -diylbis(ethyn-2,1-diyl)) bis(2,2,6,6-tetramethyl-5,6-dihydropyridin-1(2H)-(1-^{15} N)-yloxyl), biradical (B2).

To a degassed solution of **2** (281 mg, 1.0 mmol) in THF (20 mL) and Et_3N (2.5 mL), CuI (20 mg, 0.1 mmol), and Pd $(PPh_3)_4$ (50 mg, 0.04 mmol) were added under N_2 and after stirring for 15 min, compound **5** (354 mg, 1.0 mmol) in THF (5 mL) was added dropwise. After stirring the mixture overnight at room temperature, it was filtered through Celite, the solvent was evaporated and the residue was dissolved in CH_2Cl_2 (20 mL), washed with brine (10 mL), the organic phase was separated, dried ($MgSO_4$), activated MnO_2 (86 mg, 1.0 mmol) was added, and O_2 was bubbled for 15 min. The mixture was set aside for 6 h, then filtered, evaporated and the residue was purified by flash column chromatography (hexane/CH_2Cl_2) to yield compound **B2** 126 mg (25%) as yellow solid, mp 230–232 °C, R_f: 0.25 (hexane/Et_2O, 2:1). IR = 1650 cm^{-1} (C=C), MS (70 eV): *m/z* = 507 (M^+, 17), 477 (45), 462 (46), 446 (55), 431(49), 165 (100). Anal. Calcd. for $C_{34}H_{38}{}^{15}NNO_2$: C, 80.44; H, 7.54; N, 5.71. Found: C, 80.31; H 7.55; N, 5.68.

2.4 4,4′-([1,10 -Biphenyl]-4,4′ -diylbis(ethyn-2,1-diyl)) bis(2,2,6,6-tetramethyl-5,6-dihydropyridin-1(2H)- (1-^{15} N)-(1′-^{15} N)-yloxyl) Biradical (B3)

To a degassed solution of **2** (281 mg, 1.0 mmol) in THF (20 mL) and Et_3N (2.5 mL), CuI (10 mg, 0.05 mmol) and Pd $(PPh_3)_4$ (25 mg, 0.02 mmol) were added under N_2 and after stirring for 15 min, compound **3** (101 mg, 0.5 mmol) in THF (5 mL) was added dropwise. After stirring the mixture overnight at room temperature, it was filtered through Celite, the solvent was evaporated and the residue was dissolved in CH_2Cl_2 (10 mL), washed with brine (5 mL), the organic phase was separated, dried ($MgSO_4$), activated MnO_2 (86 mg, 1.0 mmol) were added, and O_2 was bubbled for 15 min. The mixture was set aside for 6 h, then filtered, evaporated and the residue was purified by flash column chromatography (hexane/CH_2Cl_2) to yield compound **B3** 55 mg (21%), as a deep yellow solid mp 230–232 °C, R_f: 0.25 (hexane/Et_2O, 2:1). IR = 1650 cm^{-1} (C=C), MS (70 eV): m/z = 508 (M^+, 13), 493 (25), 478 (17), 463 (32), 447 (21), 42 (100). Anal. Calcd. for $C_{34}H_{38}{}^{15}N_2O_2$: C, 80.28; H, 7.53; N, 5.90. Found: C, 80.33; H, 7.48; N, 5.75.

Reagents and conditions: (a) $N_2H_4 \cdot H_2O$ (6 equiv.), EtOH, rt → reflux, 1 h, then PbO_2, O_2, then TMG (3.5 equiv.), I_2 (2.0 equiv.), THF, rt., 2 h, 30%; (b) **3** (3 equiv.), **4** (1 equiv.), CuI, Pd$(PPh_3)_4$ (cat.), Et_3N (excess), THF, rt., 3 h, 31% (**5**), 33% (**B1**); (c) **2** (1 equiv.), **5** (1 equiv.), CuI, Pd$(PPh_3)_4$ (cat.), Et_3N (excess), THF, rt., 8 h, 25% (**B2**); (d) **3** (1 equiv.), **2**(2 equiv.), CuI, Pd$(PPh_3)_4$ (cat.), Et_3N (excess), THF, rt., 8 h, 21% (**B3**).

2.5 EPR Measurements

EPR measurements were performed on an Elexsys E580 spectrometer (Bruker) at X-band. The spectrometer was equipped with a commercially available cavity of

Flexline series ER4118MD5 (X). The cavity was inserted into the CF935 cryostat. Temperatures were controlled by an ITC503 temperature control system.

For liquid phase measurements, toluene was selected as a low-viscosity solvent in which all biradicals are well dissolved. It was carefully purified according to the literature procedure [27]. Solutions were prepared, bubbled with nitrogen for 20–25 min, 0.5 ml of a solution was taken into a thin glass capillary and degassed by freeze-pump cycle three times to remove oxygen, and sealed off under vacuum. Radical concentrations were sufficiently low ($\lesssim 4\times10^{-4}$ mol l^{-1}) to eliminate intermolecular exchange broadening of EPR lines [8].

Continuous-wave EPR spectra of the biradicals at liquid phase were simulated using the approach described in [1]. For our calculations, we used spin-Hamiltonian parameters of similar nitroxide radicals collected in [28].

3 Theoretical Background

A theory of the EPR spectra of nitroxide biradicals with ^{14}N isotopes is given in detail in [1]. In the case of a low-viscosity medium, the anisotropic interactions, e.g., dipole–dipole interactions between two unpaired electrons of a biradical and those between unpaired electrons and magnetic nuclei are effectively averaged to zero due to fast enough rotational diffusion of biradicals. Then the EPR frequencies are determined by the isotropic spin-Hamiltonian

$$\boldsymbol{H} = h(\nu_0\left(\boldsymbol{S}_z^{(1)} + \boldsymbol{S}_z^{(2)}\right) + \left(a_1\boldsymbol{S}_z^{(1)}\boldsymbol{I}_z^{(1)} + a_2\boldsymbol{S}_z^{(2)}\boldsymbol{I}_z^{(2)}\right) + J\boldsymbol{S}^{(1)}\boldsymbol{S}^{(2)} - (\nu_{n1}\boldsymbol{I}_z^{(1)} + \nu_{n2}\boldsymbol{I}_z^{(2)})). \tag{1}$$

Here ν_0, ν_n are the Zeeman frequencies of unpaired electrons and nitrogen nuclei, respectively, e.g., $\nu_0 = g\beta_e H_0/h$, a is the constant of the isotropic hyperfine interaction (HFI) of unpaired electrons with nitrogen nuclei, J is the exchange integral. Superscripts 1 and 2 denote different radical centers; $\boldsymbol{S}^{(k)}$ are electron spin operators; $\boldsymbol{S}_z^{(k)}$ and $\boldsymbol{I}_z^{(m)}$ are projections of the electron and nitrogen nuclear spins operators to the Z axis, respectively; g is the isotropic g-factor of the radicals; β_e is the Bohr magneton;H_0 is the external magnetic field induction; h is the Planck constant.

Note that we did not include the isotropic HFI of the unpaired electrons with protons and ^{13}C nuclei into the spin-Hamiltonian Eq. (1). Typically, these HFI are an order of magnitude less than the HFI with nitrogen nuclei in nitroxide biradicals [28]. We assume that there are EPR lines induced by the HFI with nitrogen nuclei, while other nuclei inhomogeneously broaden "nitrogen" components of the EPR spectrum. In principle, all HFI terms can be easily included into consideration. However, to highlight some characteristic features of EPR spectra of biradicals discussed below, the minor interactions with protons, which are small in comparison with the major splitting of the biradicals EPR spectrum by the HFI with nitrogen nuclei, can be omitted.

In the case of the spin-Hamiltonian Eq. (1), Z-projections of nuclear spins do not change in time. This fact makes it possible to divide a given ensemble of nitroxide biradicals into sub-ensembles of biradicals with fixed projections of nuclear spins

M_1 and M_2. For nuclear spin $I=1$ (^{14}N isotope) $M_k=\{1, 0, -1\}$, and for nuclear spin $I=1/2$ (^{15}N isotope) $M_k=\{1/2, -1/2\}$, $k=1, 2$.

In this situation, the EPR frequencies of sub-ensemble of biradicals with fixed $\{M_1, M_2\}$ are determined by the spin-Hamiltonian

$$\boldsymbol{H} = h((\nu_0 + a_1 M_1)\boldsymbol{S}_z^{(1)} + (\nu_0 + a_2 M_2)\boldsymbol{S}_z^{(2)} + J\boldsymbol{S}^{(1)}\boldsymbol{S}^{(2)}) \tag{2}$$

For the spin-Hamiltonian Eq. (2), in each sub-ensemble of biradicals two radical centers have resonance frequencies

$$\begin{aligned} \nu_1 &= \nu_0 + a_1 M_1, \\ \nu_2 &= \nu_0 + a_2 M_2. \end{aligned} \tag{3}$$

When $\nu_1 = \nu_2$, the unpaired electrons of two radical centers become magnetically equivalent. This situation occurs in the case of symmetric nitroxide biradicals when $a_1 = a_2$ for sub-ensembles of biradicals with equal projections of nitrogen nuclear spins $M_1 = M_2$. The exchange interaction is not manifested in the EPR spectra of these sub-ensembles of biradicals with magnetically equivalent radical centers. Thus, the EPR spectrum of the symmetric biradicals always lines with the resonance frequencies

$$\nu = \nu_0 + aM, M = I, I-1, \ldots, -I, \tag{4}$$

which coincide with the resonance frequencies of individual radicals. It follows that the EPR spectra of these sub-ensembles of biradicals do not make it possible to determine the exchange integral for these sub-ensembles of biradicals.

The exchange interaction is manifested in the EPR spectrum in sub-ensembles of biradicals with magnetically non-equivalent radical centers. They are implemented for symmetric biradicals when projections of nitrogen nuclear spins are not equal $M_1 \neq M_2$.

In the case of asymmetric biradicals, when $a_1 \neq a_2$, the unpaired electrons of the two interacting radicals are magnetically non-equivalent independent of the projections of nitrogen nuclear spins, M_1 and M_2.

For biradicals with the spin-Hamiltonian Eq. (1), the EPR spectrum is a sum of the EPR spectra of sub-ensembles of biradicals with given projections of the spins of nitrogen nuclei (see Eq. 2). In the presence of the exchange interaction (see Eq. 2), the EPR spectrum of sub-ensembles of biradicals with magnetically non-equivalent radical centers changes specifically as a function of the ratio q of the splitting of two lines and the exchange integral:

$$q = \left|J/\left(\nu_1 - \nu_2\right)\right| = \left|J/\left(a_1 M_1 - a_2 M_2\right)\right| \tag{5}$$

The EPR spectra of the sub-ensembles of biradicals, which have magnetically non-equivalent radical centers, have two "nitrogen" components in their EPR spectra without the exchange interaction ($J = 0$), since $\nu_1 \neq \nu_2$ (see Eq. 3). In the case of $\nu_1 \neq \nu_2$, the exchange interaction is manifested: it splits each component into a doublet. The features of this splitting depend on the parameter q (5). When the

exchange interaction is small compared with the distance between two EPR spectrum components, so that $q \ll 1$, the exchange interaction can be reduced to a secular spin-Hamiltonian

$$H_{ex} = hJS_z^{(1)}S_z^{(2)} \tag{6}$$

Under these conditions, each EPR nitrogen hyperfine structure component splits into two components with resonance frequencies $(\nu_k + J/2)$ and $(\nu_k - J/2), k = 1,2$ (see Eq. 3). This splitting is symmetric with respect to ν_k only in the approximation linear over the parameter q (see Eq. 7).

For the arbitrary J value, the sub-ensemble of biradicals with the spin-Hamiltonian Eq. (2) has the EPR resonance frequencies $\{\nu_k\}$ and intensities S_1, S_2 of corresponding resonance lines as given by Eq. (7)

$$\begin{aligned}
E_1 &= \tfrac{\nu_1}{2} + \tfrac{\nu_2}{2} - \tfrac{J}{2} - \tfrac{1}{2}\sqrt{(\nu_1-\nu_2)^2 + J^2}; S_1 = S_0\left(\tfrac{1}{4} - \frac{J}{4\sqrt{(\nu_1-\nu_2)^2+J^2}}\right);\\
E_2 &= \tfrac{\nu_1}{2} + \tfrac{\nu_2}{2} + \tfrac{J}{2} - \tfrac{1}{2}\sqrt{(\nu_1-\nu_2)^2 + J^2}; S_2 = S_0\left(\tfrac{1}{4} + \frac{J}{4\sqrt{(\nu_1-\nu_2)^2+J^2}}\right);\\
E_3 &= \tfrac{\nu_1}{2} + \tfrac{\nu_2}{2} - \tfrac{J}{2} + \tfrac{1}{2}\sqrt{(\nu_1-\nu_2)^2 + J^2}; S_2 = S_0\left(\tfrac{1}{4} + \frac{J}{4\sqrt{(\nu_1-\nu_2)^2+J^2}}\right);\\
E_4 &= \tfrac{\nu_1}{2} + \tfrac{\nu_2}{2} + \tfrac{J}{2} + \tfrac{1}{2}\sqrt{(\nu_1-\nu_2)^2 + J^2}; S_1 = S_0\left(\tfrac{1}{4} - \frac{J}{4\sqrt{(\nu_1-\nu_2)^2+J^2}}\right);
\end{aligned} \tag{7}$$

The exchange interaction splits the resonance lines at frequencies ν_1 and ν_2 into doublets with frequencies $\{E_1, E_2\}$ and $\{E_3, E_4\}$. For the arbitrary J value, the splitting of lines into these doublets is asymmetric with respect to ν_k (Fig. 2). The splitting of two doublet lines is $E_2 - E_1 = E_4 - E_3 = J$ (see Eq. 7).

The lines with frequencies E_1 and E_4 have intensities S_1, while the lines with frequencies E_2 and E_3 have intensities S_2 (see Eq. 7). According to Eq. (7), $S_2 \geq S_1$, when $J > 0$, and vice versa, when $J < 0$.

When $J \to \infty$, the components of the doublets with intensities S_2 tend to the center of gravity of ν_1 and ν_2 frequencies, $\nu_{av} = (\nu_1 + \nu_2)/2 \equiv \nu_0$. The intensity S_2 tends to the limit S_0 value.

At the same time, other lines of these doublets go far away infinitely. The intensity S_1 tends to zero and these components of the spectrum become forbidden. This occurs because the triplet and singlet states become eigenstates of two unpaired electrons in the biradical for large enough exchange integral. As a result, when $J \to \infty$, only the resonance in the triplet state with the frequency ν_0 is manifested in the EPR spectrum.

Note that even at $J \to \infty$, the EPR spectrum of the total ensemble of all biradicals is not reduced to one line with the frequencyν_0. Sub-ensembles of biradicals with magnetically non-equivalent radical centers, which have different configurations of nuclear spins $\{M_1, M_2\}$, have their own average frequency at $J \to \infty$

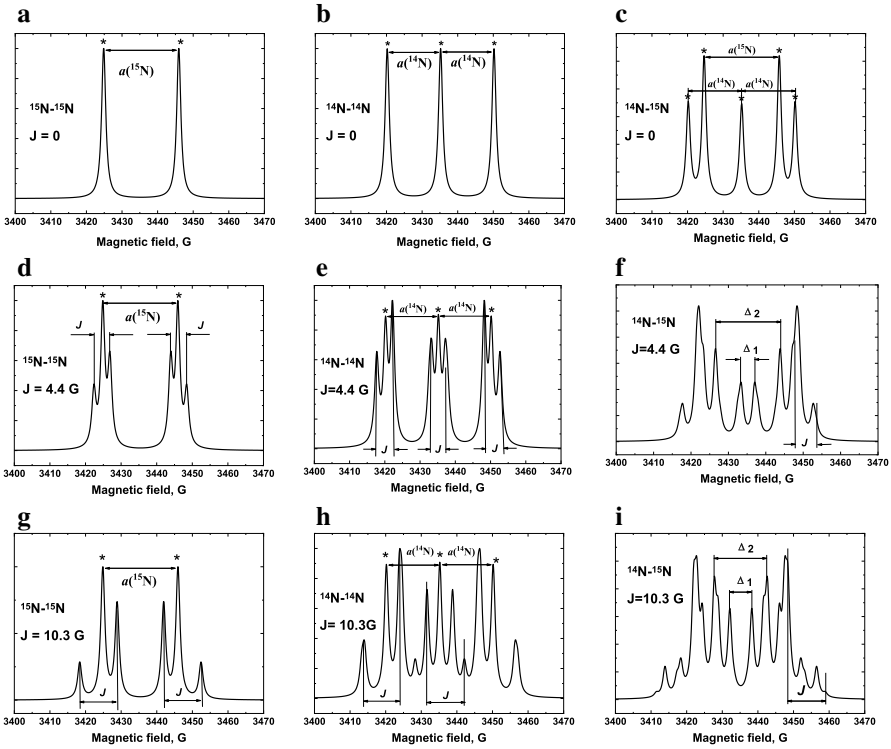

Fig. 2 Calculated EPR spectra of biradicals containing ^{15}N/^{15}N [left-hand column (**a**, **d**, **g**)], ^{14}N/^{14}N [central column (**b**, **e**, **h**)], and ^{14}N/^{15}N [right-hand column (**c**, **f**, **i**)] pairs for different exchange integral values: J=0 [upper row (**a**–**c**)]; J =4.4 G [middle row (**d**, **e**, **f**)]; J =10.3 G [down row (**g**–**i**)]. HFI constants are $a(^{15}\mathrm{N})=21$ G and $a(^{14}\mathrm{N})=15$ G. $\Delta_1 = \left|J + a(^{15}N) - \sqrt{J^2 + (a(^{15}N)/2)^2}\right|$ and $\Delta_2 = \left|J - a(^{15}N) - \sqrt{J^2 + (a(^{15}N)/2)^2}\right|$. The asterisk marks the lines corresponding to the HFI with nitrogen nuclei of monoradicals. Note that to convert J and a from Gauss into rad/s they are to be multiplied by the factor of 1.76×10^7. The form of each resonance line is a Lorentzian absorption curve. The width of all Lorentzian lines is 1.4 G

$$\nu_{av}(M_1, M_2) = \nu_0 + (a_1 M_1 + a_2 M_2)/2 \tag{8}$$

In fact, for a given sub-ensemble of biradicals with magnetically non-equivalent radical centers, at any large but not infinite J value, there are two close resonance lines with the following frequencies around the average frequency Eq. (8) (see Eqs. 7, 8).

$\nu_{av} - \frac{(\nu_1-\nu_2)^2}{4|J|}$ and $\nu_{av} + \frac{(\nu_1-\nu_2)^2}{4|J|}$. The splitting of these two lines is $\triangle\nu = \frac{(\nu_1-\nu_2)^2}{2|J|} \to 0$ when $J \to \pm\infty$.

It was pointed out above that in the case of symmetric nitroxide biradicals, there are sub-ensembles of biradicals with $M_1 = M_2 = M$, the EPR frequencies of which are not affected by the exchange interaction. These biradicals contribute

the resonance lines with frequencies not disturbed by the exchange interaction to the spectrum of biradicals

$$\nu_{nd} = \nu_0 + aM, M = I, I-1, \ldots, -I \tag{9}$$

These speculations are illustrated by the results of calculations of resonance frequencies of nitroxide biradicals using the spin-Hamiltonian Eq. (2), when the exchange integral changes (Fig. 2).

The model spectra of nitroxide biradicals shown in Fig. 2 illustrate the characteristic manifestations of the isotope substitution and the value of the exchange interaction in the form of the EPR spectrum expected according to theoretical consideration presented above (Eqs. 1–9). It is assumed in the calculations that a certain conformation of the nitroxide biradical is taken and the exchange integral J of the interaction of the radical centers is given.

Naturally, at $J = 0$, the EPR spectrum of biradicals coincides with the sum of the spectra of individual (non-interacting) radicals (see the upper row of the spectra in Fig. 2).

In the case of biradicals with $J \neq 0$, the resonance lines of individual radicals are observed only for biradicals with magnetically equivalent unpaired electrons.

- This situation is possible for symmetric biradicals under the additional condition of equal projections of the nuclear nitrogen spins in both radical centers of the biradical (see Eq. 9) $M_1 = M_2$. The corresponding lines in the spectrum are marked with an asterisk in Fig. 2.
- In the asymmetric biradical $^{14}N/^{15}N$ at $J \neq 0$, the lines at the frequencies of individual radicals in the spectrum are not expected, since in this case situations with magnetically equivalent unpaired electrons of two radical centers cannot be implemented (see spectra in the right-hand column in the middle and down rows in Fig. 2).

In sub-ensembles of biradicals with magnetically nonequivalent unpaired electrons of radical centers, the inclusion of the exchange interaction splits the spectrum lines into two lines (compare, e.g., the spectra in the upper and middle rows in Fig. 2).

- In the case of symmetric biradicals, such sub-ensembles are the biradicals, in which the projections of the nuclear nitrogen spins in the radical centers differ, $M_1 \neq M_2$ (see spectra in the left-hand and middle rows in Fig. 2).
- In the case of asymmetric biradicals, all sub-ensembles are magnetically nonequivalent (see spectra in the right-hand column in Fig. 2)

The spectra in Fig. 2 also show clearly that the splitting of the spectrum lines in the ensembles of biradicals with magnetically nonequivalent unpaired electrons of radical centers is asymmetric. In the sub-ensemble of biradicals with the exchange integral J, the difference in the resonance frequencies of the two lines of the doublet is J (Eq. 7). The corresponding splitting of lines in doublets are marked in Fig. 2.

Thus, the positions of the lines in the spectra of biradicals make it relatively easy to determine the HFI constants and exchange integrals in the ensembles of biradicals with different conformations. Of course, it is necessary to take into account the shift in the positions of the maxima of individual lines of the spectrum due to the overlap of different lines.

The shapes of individual resonance lines were approximated as Lorentzians in these calculations. In fact, each nitrogen HFI component in the EPR spectrum of nitroxide radicals has inhomogeneous broadening due to the HFI with protons. The real shape of the nitrogen components of spectra of individual radicals should be presented as a convolution of Lorentzian spin packets line shape and the distribution of resonance frequencies of these spin packets due to the HFI with protons [29]. In our approximation, the inhomogeneously broadened nitrogen HFI components are presented as "homogeneously" broadened lines with some effective widths. The intensities of the line wings are overestimated if the Lorentzian approximation is used.

When interpreting the EPR spectra of biradicals, it is necessary to keep in mind that biradicals may have several conformations with different distances between two radical centers, different electron spin density distributions, different HFI constants, and different exchange integrals. An important issue is that any isotope substitution affects only the HFI constants for all possible conformations of biradicals. Moreover, the HFI constants change only due to the change in the gyromagnetic ratios of isotope nuclei and quantum numbers of isotope nuclear spins. The isotope substitution is a useful instrument to study the structure of biradicals and their transitions between different conformations [1].

In the case of several conformations, the total EPR spectrum is a sum of spectra of biradicals with different magnetic resonance parameters, e.g., J and a. This additive approach is justified if the conformational transitions are slow enough. In the general case, the EPR spectrum is affected by the conformational transitions. For example, the conformational transitions shorten the lifetime of the electron spin with a definite spin-Hamiltonian related to one of the conformations. This leads to broadening of EPR lines similar to broadening of EPR lines in the course of chemical exchange. We will consider this problem below.

4 Results and Discussion

4.1 EPR Spectra

Figure 3 shows the experimental and calculated spectra of the asymmetric biradical **B2** (Fig. 3c), and the symmetric biradical **B3** (Fig. 3a). The EPR spectrum of the symmetric biradical **B1** (Fig. 3b) [22] is shown to be of help in the analysis of the EPR spectrum of the asymmetric biradical **B2**.

Figure 3 shows two simulated EPR spectra for each of the biradicals (Sim1 and Sim2). The first simulation (Sim1) was done under the assumption that there is only one configuration of biradicals with the exchange interaction between the radical fragments of 4.4 G. This simulation describes well the positions of the intense lines

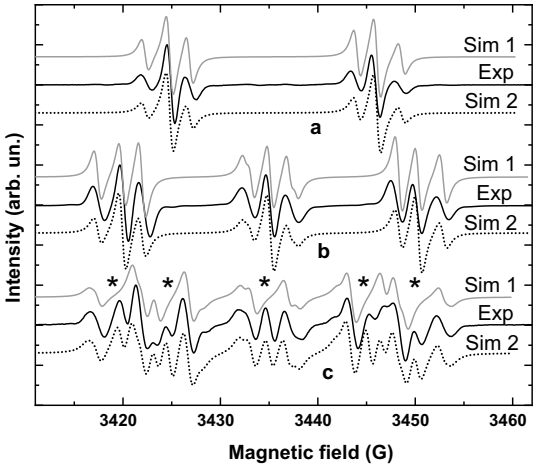

Fig. 3 Experimental (Exp) and simulated (Sim) EPR spectra of biradicals **B1** (b), **B2** (c) and **B3** (a). Experimental spectra measured at 300 K are shown by thick curves. Thin curves show spectra calculated at the assumption that all biradicals exist in only one conformation with $|J| = 4.4$ G (Sim1). Dashed curves present the case of two conformations with $J_1 = 0$ and $|J_2| = 4.4$ G, while their statistic weights are $p_{J=0} = 0.285$ and $p_{|J|=4.4G} = 0.715 = 1 - p_{J=0}$, respectively (Sim2) b Exp adapted from [22] with the permission of Springer)

for the biradicals **B1** and **B3**, but does not describe some lines for the biradical **B2**. These lines are marked with an asterisk in Fig. 3. It should be noted that these lines correspond exactly to the line positions in the EPR spectrum due to the HFI with nitrogen nuclei (compare with asterisks in Fig. 2). The presence of these lines indicates that there are biradicals in the system, in which the exchange interaction is zero (see the upper row of EPR spectra in Fig. 2). The second simulation of the EPR spectra (Sim2) was done taking into account that there are two conformations of biradicals in the system with $J_1 = 0$ and $|J_2| = 4.4$ G. It can be seen that the second simulation describes qualitatively the experimental EPR spectra much better.

To discuss the properties of biradicals, the EPR spectra are more instructive than their derivatives (Fig. 3). The latter are also called EPR spectra. Figure 4 shows the spectra obtained by integrating the derivative spectra shown in Fig. 3.

The shapes of the EPR spectra (Figs. 3 and 4) allow several observations: the splitting of the experimental lines indicate the exchange interaction between radical centers. Moreover, there are biradicals with different exchange integrals. This means that biradicals under study have several conformations.

For all biradicals, there are resonance lines which correspond to resonance lines for isolated radicals and have no splitting. It was shown above that this observation is expected for the arbitrary exchange interaction in case of symmetric biradicals **B1** and **B3** with magnetically equivalent unpaired electrons of two radical centers (see Fig. 2, the first and second columns and discussion in text). In the case of the asymmetric biradical **B2,** this observation is not expected for the arbitrary exchange integral. It occurs only in the presence of biradicals with the zero exchange interaction (see Fig. 2, spectra in the third column).

The possible conformations of biradicals **B1**, **B2**, **B3** and populations of their different conformations should coincide within the Born–Oppenheimer approximation.

Keeping this in mind, first, we analyze the EPR spectrum of the "simplest" biradical **B3** in detail (see Figs. 3a, 4a). In this case, the EPR spectrum consists of two groups of lines. Each of the nitrogen components is split due to the exchange

Fig. 4 Non-derivative EPR spectra of biradicals **B1** (**b**, **c**), **B2** (**d**–**g**), and **B3** (**a**) studied at 300 K: the ▶ experimantal spectra are shown by thin curves, simulated one are shown by thick curves. Parameters of simulation: (**a**, **b**, **d**) {67.5% at $|J| = 4.4$G; 27.5% at $J = 0$; 3% at $|J| = 11.2$G; 2% at $|J| = 57.0$G}; **c** {79.0% at $|J| = 4.4$G; 16% at $J = 0$; 3% at $|J| = 11.2$G; 2% at $|J| = 57.0$G}; **e** {63% at $|J| = 4.4$G; 32% at $J = 0$; 3% at $|J| = 11.2$G; 2% at $|J| = 57.0$G}; **f** ($*\alpha$ (**B2**) = 0.8; β(**B1**) = 0.2.*) {78.0% at $|J| = 4.4$G; 17% at $J = 0$; 3% at $|J| = 11.2$G; 2% at $|J| = 57.0$G}; **g** ($*\alpha$ (**B2**) = 0.8; $\beta(^{14}N) = 0.2$.*) {78.0% at $|J| = 4.4$G; 17% at $J = 0$; 3% at $|J| = 11.2$G; 2% at $|J| = 57.0$G}

interaction. The EPR spectrum of the symmetric biradical **B3** shows that there are four conformations. Best fitting of the EPR spectrum was found using the isotropic HFI constant $a(^{15}\text{N}) = 21$ G. There are sub-ensembles of biradicals with the exchange integrals $|J| = \{0;4.4;11.2;57.0\}$ G, while their populations relate as 0.27:0.68:0.03:0.02, respectively. The ground state of the biradicals has the conformation with $|J| = 4.4$ G. The effective linewidth used in the fitting procedure was chosen as 1.4 G.

Thus, there is a mixture of biradicals with the zero exchange interaction (27% of content), weak exchange interaction $|J| < a(^{15}\text{N})$ (68%), strong exchange interaction $|J| > a(^{15}\text{N})$ (2%), and intermediate exchange interaction (3%).

The EPR spectrum of the biradical **B1** was simulated using parameters obtained for the biradical **B3** (see Figs. 3b, 4b, c). Note that the isotropic HFI constant $a(^{14}\text{N}) = 15$ G was found as $a(^{14}\text{N}) = a(^{15}\text{N})$ ($\gamma(^{14}\text{N})/\gamma(^{15}\text{N})$), where γ are gyromagnetic ratios for the corresponding isotope nuclear spins. The equation arises from the fact that the isotope substitution does not change the electron spin density distribution in radical centers.

It was expected that the biradical **B1** has the same relative content of different conformations 0.27:0.68:0.03:0.02 as for the biradical **B3**. The EPR spectrum simulated under this assumption is shown in Fig. 4b. Better fitting was achieved for slightly different ratios of sub-ensembles of biradicals with different exchange interactions shown in Fig. 4c. In this case, the relative content of different conformations is 0.16:0.79:0.03:0.02.

In accordance with thermodynamics, the ratio of populations of conformations with $J = 0$ and $|J| = 4.4$ G should be the same. However, the best fitting of the EPR intensities given in Fig. 4a,c suggest different ratios of 0.27:0.68 and 0.16:0.79 for conformations with $J = 0$ and $|J| = 4.4$ G for biradicals **B3** and **B1**, respectively. This contradiction can be resolved if it is assumed that there are radicals which are not coupled into biradicals. From the EPR spectroscopy point of view, a biradical with $J = 0$ gives the same contribution to the EPR spectrum as two individual radicals. Under this condition, it is possible even to suggest that there are no biradicals with $J = 0$ at all. A sub-ensemble of biradicals with $J = 0$ can be considered as a new sub-ensemble of individual radicals. It is shown below that there is a temperature dependence of the EPR spectrum shape and its interpretation assumes that there should be biradicals with $J = 0$. Keeping this in mind, we interpret the results shown in Fig. 4a–c that in the cases of biradicals **B1** and **B3,** there are biradicals with $J = 0$ and monoradicals simultaneously.

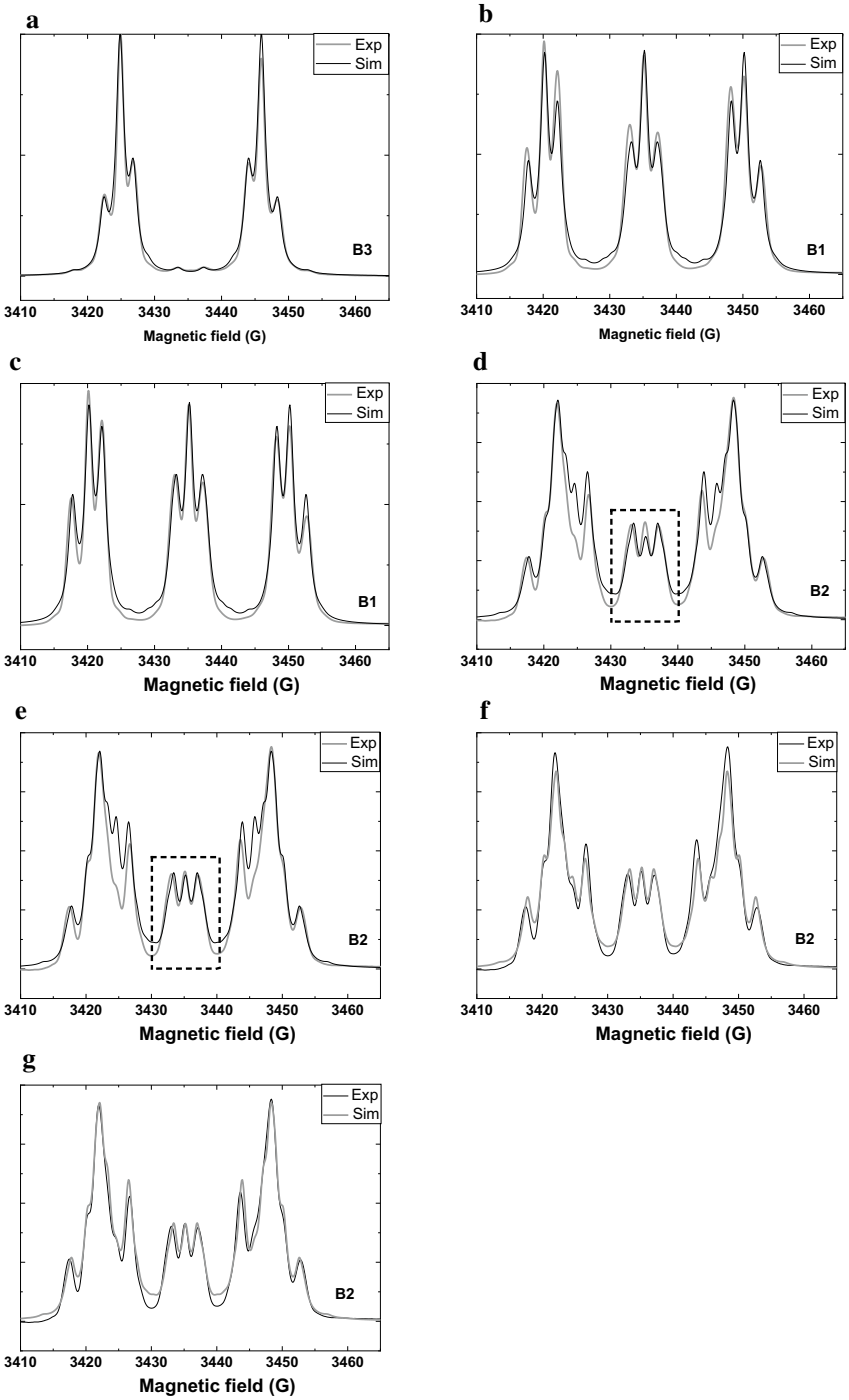
a
Exp
Sim
B3
3410 3420 3430 3440 3450 3460
Magnetic field (G)
b
Exp
Sim
B1
3410 3420 3430 3440 3450 3460
Magnetic field (G)
c
Exp
Sim
B1
3410 3420 3430 3440 3450 3460
Magnetic field (G)
d
Exp
Sim
B2
3410 3420 3430 3440 3450 3460
Magnetic field (G)
e
Exp
Sim
B2
3410 3420 3430 3440 3450 3460
Magnetic field (G)
f
Exp
Sim
B2
3410 3420 3430 3440 3450 3460
Magnetic field (G)
g
Exp
Sim
B2
3410 3420 3430 3440 3450 3460
Magnetic field (G)

However, the discrepancy between data concerning **B1** and **B3** biradicals may be the result of the erroneous simulation, since the effect of the HFI with protons was taken into account phenomenologically rather than theoretically consistent.

Figures 3c and 4d–g show the EPR spectrum for the asymmetric biradical **B2**. The position of the lines of this spectrum are described well using the exchange integrals and HFI constants, which have been already determined when studying biradicals **B1** and **B3**. This is the expected result.

Figure 4d shows the result of fitting the EPR spectrum of the biradical **B2** under the assumption that it has the same relative content of different conformations 0.27:0.68:0.03:0.02 as for the biradical **B3**. Best fitting of the relative intensities of the central triplet band in the experimental EPR spectrum is obtained at slightly different relative content of different conformations of 0.32:0.63:0.02:0.03 (Fig. 4e).

Our attempts to present the experimental EPR spectrum as a sum of the calculated EPR spectra of asymmetric **B2** biradicals in conformations with $|J| = \{0, 4.4, 11.2, 57\}$ G were unsuccessful. In all cases, with different ratios of content of configurations, the simulated spectra very poorly describe the region of the experimental EPR spectrum that is related to radical centers with the ^{15}N nitrogen isotope (Fig. 5d, e). The discrepancy between the calculated spectra and the observed spectrum indicates that the content of radicals with ^{14}N and ^{15}N isotopes in this system differs, i.e., in addition to the asymmetric biradical **B2**, there are other particles in the studied system. In principle, these can be symmetrical biradicals and/or monoradicals.

In fact, the EPR spectrum detected in the system containing asymmetric biradicals definitely indicate that the number of radical centers with ^{14}N and ^{15}N containing radicals are different. There should be more ^{14}N radicals than ^{15}N radicals. This statement results from two observations:

- In Fig. 4d, e the intensities of the experimental EPR lines are noticeably less than intensities of the simulated spectra for the lines, which correspond to resonances of the ^{14}N containing radicals (compare experimental and simulated spectra in Fig. 4d, e).

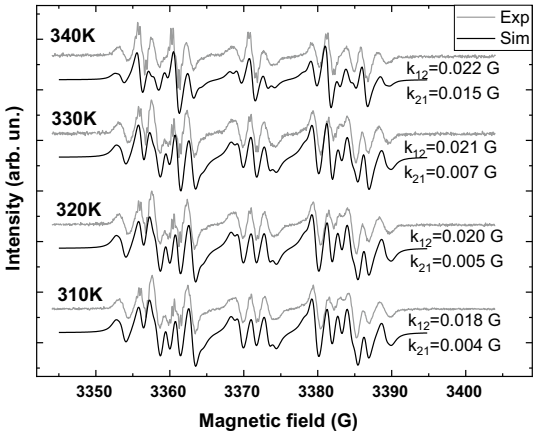

Fig. 5 Experimental (gray) and theoretical (black) EPR spectra of **B2** at different temperatures. Fitting of calculated spectra is done under assumption that biradicals have two conformations with $J = 0$ (state 1) and $|J| = 4.4$ G (state 2) and the chemical exchange between these conformations occurs

- Integrated intensities of different parts of the EPR spectrum show that there is an excess amount of ^{14}N radicals in the studied system.

According to the above results (Fig. 2), the main electronic state in the studied biradicals is the configuration with the exchange integral $|J|$=4.4 G. This exchange integral is less than the HFI constants of unpaired electrons with magnetic nuclei of nitrogen isotopes. Under these conditions, three lines in the center of the spectrum, highlighted in Fig. 4d, e dotted, give the full contribution to the EPR spectrum of all ^{14}N radicals whose nitrogen nuclear spin projection is $M=0$. Therefore, we can do the following: we calculate the integral intensity of the selected part of the spectrum registered in the experiment in the center of the spectrum. This number is equal in conventional units $I_c=1$. The parts of the EPR spectrum to the left and right of the part highlighted in the center belong to the ^{14}N radicals, whose nuclear spin projection is equal to $M=\{1, -1\}$, respectively, on the one hand, and to the ^{15}N radicals, whose nuclear spin projection is equal to $M=\{1/2, -1/2\}$. The integral I_l intensity of the low-field part of the spectrum was found to be equal to $I_l=2.44$ in conventional units, while the high-field part gives $I_h=2.37$. The differences between these total intensities and the contribution intensity of one-third of the ^{15}N radicals with $M=0$, i.e., I_l-I_c and I_h-I_c give the contribution to the intensity of half of the ^{15}N radicals with projections of the nuclear spin of ½ and −½, $I_l-I_c=1.44$, $I_h-I_c=1.37$, respectively.

Thus, we get that in the same conditional units, ^{14}N radicals contribute 3*1 =3 to the integral intensity of the spectrum, and ^{15}N radicals contribute 1.44+1.37=2.81. This means that in a system containing **B2** biradicals, there are more ^{14}N radicals than ^{15}N radicals. "Excess" ^{14}N radicals can be in the state of monoradicals or enter symmetrical biradicals **B1**.

The excess content of the ^{14}N isotope may be overestimated for two reasons.

- First, it is known from the analysis of the spectra of symmetric biradicals that about 5% of biradicals have a sufficiently large exchange integral. Sub-ensembles of asymmetric biradicals with large exchange integral values can contribute to the integral intensity of the selected part in the center of the spectrum. Therefore, the above value $I_c=1$ overestimates the contribution of ^{14}N radicals with the nuclear spin projection $M=0$.
- Second, there is the effect of overlapping lines. It can also change the above integral intensities of different sub-assemblies of biradicals. Therefore, we performed fitting of the EPR spectrum of the system with an asymmetric biradical, taking into account that there should be more ^{14}N radicals than ^{15}N one.

The examples of the best fitting assuming the excess amount of ^{14}N radical are shown in Fig. 4f, g. These curves were obtained under the assumption that 80% of all nitroxide radicals are in the asymmetric **B2** biradical state while the “excess” ^{14}N radicals are in the symmetric **B1** biradical state (Fig. 4f) or the monoradical state (Fig. 4g).

The comparison of simulated spectra in Fig. 4d–g shows that taking into account of excess ^{14}N radicals leads to much better fitting of the experimental EPR spectrum.

Thus, the analysis of the EPR spectra at $T = 300$ K allows the following conclusions:

- The EPR spectra of radicals **B2** and **B3** and the EPR spectrum of the radical **B1** [22] show that there are four conformations, in which the exchange integral is 0, 4.4 G, 11.2 G and 57 G in all these nitroxide biradicals.
- Biradicals having the conformation with $|J| = 4.4$ G make the major contribution to the experimental EPR spectrum. This means that the conformation with $|J| = 4.4$ G is the ground electronic term for the studied biradicals.
- Biradicals having the conformations with $|J| = 11.2$ G or 57 G give 2–3% of the intensity of the experimental EPR spectrum.
- The EPR data provide an estimate of the relative populations of two most populated conformations of biradicals with $|J| = 4.4$ G and $J = 0$. The ratio p ($|J| = 4.4$ G):p($J = 0$) is about 4:1 at room temperatures.

It was pointed out above that the analysis of the EPR spectra of biradicals at one temperature does not make it possible to unequivocally state the presence of biradicals with $J = 0$, since their EPR spectrum coincides with the sum of the spectra of two monoradicals forming a biradical. However, EPR spectroscopy has the resource to prove the presence of biradicals with $J = 0$. To this end, it is necessary to study experimentally, the EPR spectra at different temperatures.

As the temperature changes, the ratio of biradicals with different configurations changes, and this changes the ratio of the contributions of biradicals with different exchange integrals to the EPR spectrum. This "chemical exchange" between conformations characteristically changes the shape of the EPR spectra of biradicals as well: it causes the shift in the resonance frequencies and changes the width of the observed resonance lines [1]. For example, in the field of slow chemical exchange (relatively slow conformational transitions in a biradical), the lifetime of biradicals in one or another conformation is reduced. This in turn leads to a broadening of the resonance lines due to the uncertainty principle for the energy levels of spins in the biradical and the lifetime of the biradical in a given configuration.

The experimental EPR spectra at several temperatures are shown in Fig. 5.

Figure 5 also shows best fitting of the EPR spectra. When simulating the temperature dependence of the spectra we took into account only two conformations of biradicals: with $|J| = 4.4$ G and $J = 0$. We expect that taking into account also the conformations with $|J| = 11.2$ G and $|J| = 57$ G will not change drastically the results since their content is minor, of 2–3% only.

To simulate the spectrum shape in the presence of chemical exchange, we used the well-known approach [1]. We introduce spin density matrices ρ_1 and ρ_2, which describe the states of electron spins of biradicals in conformations with $J = 0$ or $|J| = 4.4$ G, respectively. The spin dynamics in the presence of conformation transitions is described by equations

$$\begin{aligned}\partial\rho_1/\partial t &= -i/h\big[H(1),\rho_1\big] - R_{rel}\rho_1 - K_{12}\rho_1 + K_{21}\rho_2,\\ \partial\rho_2/\partial t &= -i/h\big[H(2),\rho_2\big] - R_{rel}\rho_2 + K_{12}\rho_1 - K_{21}\rho_2,\end{aligned} \tag{10}$$

where $H(k)$, $k = 1,2$, is the spin-Hamiltonian given by Eq. (2) for $J = 0$ (state 1) and $|J| = 4.4$ G (state 2) plus the spin-Hamiltonian of the interaction of electron spins with the microwave field. The operator R_{rel} describes the relaxation of spin level populations and the relaxation of the transverse spin components within Bloch equations. Last two terms in Eq. (10) describe the effect of the chemical exchange: K_{12} is the rate constant of the monomolecular transition of the biradical from the conformation with $J = 0$ to the conformation with $|J| = 4.4$ G; K_{21} is the rate constant of the reverse monomolecular reaction.

The continuous-wave EPR spectrum is calculated using the steady-state solution of Eq. (10) in the rotating frame $(\rho_k)_{st}$. The EPR signal is proportional to

$$M_y = Tr\big(\rho_{st}\big(\boldsymbol{S}_{1y} + \boldsymbol{S}_{2y}\big)\big) \tag{11}$$

where $\rho_{st} = \rho_{st}(J = 0) + \rho_{st}(|J| = 4.4G)$ and operators $\boldsymbol{S}_{1y}$ and $\boldsymbol{S}_{2y}$ are spin projection operators of two radical centers in the biradical, respectively (see spin Hamiltonians Eqs. 1 and 2).

This algorithm was used to fit EPR spectra. Best fitting of the EPR spectra and rate constants of the chemical exchange are shown in Fig. 5. Best fitting rate constants are given in units of the magnetic field induction, Gauss. To convert them to 1/s units, one has to multiply K_{12}, K_{21} in G by $1.76{\cdot}10^7$.

The comparison of the experimental and the best fitting curves shows that they coincide reasonably well. The rate constants of the chemical exchange increase when the temperature increases. In equilibrium, the ratio n_1/n_2 of the steady-state concentrations of biradicals with various conformations is equal to the equilibrium constant $K_{\text{equil}} = K_{21}/K_{12}$. According to the data given in Fig. 5, the equilibrium constant for the two-sided first order (monomolecular) reaction

$$n_1(J = 0) \underset{K_{21}}{\overset{K_{12}}{\rightleftarrows}} n_2(|J| = 4.4G)$$

takes values $K_{\text{equil}} = \{\frac{4}{18};\frac{5}{20};\frac{7}{21};\frac{15}{22}\}$ at $T = \{310$ K, 320 K, 330 K, 340 K$\}$, respectively. We see that at room temperature 300 K, 22% of biradicals **B2** have conformation with $J = 0$, while 78% of biradicals have the conformation with $|J| = 4.4$G. Note that in these calculations we neglected the contribution of about 5% biradicals in conformations with $|J| = 11.2$ G and $|J| = 57$ G. We expect that taking into account these conformations does not change considerably the ratio of populations of conformations with $J = 0$ and $|J| = 4.4$ G.

The rate constants shown in Fig. 5 make it possible to estimate the barriers for the conformation transitions. These barriers for K_{12} and K_{21} in temperature units are about $E_{a12} = 850$ K (1.7 kcal/mol) and $E_{a21} = 4300$ K (8.5 kcal/mol), respectively. The temperature dependence of the equilibrium constant K_{12}/K_{21} makes it possible to estimate the energy level difference of the conformation with $J = 0$

and $|J| = 4.4$ G. It is equal to $\Delta E = 3450$ K = 6.9 kcal/mol. These estimates correlate with the DFT results [22].

5 Conclusion

We synthesized new biradicals and found their unpaired electron spin-dependent interactions using the EPR spectroscopy methods. These biradicals were similar to biradicals **B1** studied in [22]. Here we studied biradicals **B2** and **B3** containing rare nitrogen isotope (^{15}N/^{14}N and ^{15}N/^{15}N). The isotope substitution provides a new "degree of freedom" for studying properties of biradicals.

Under the isotope substitution, the EPR spectrum of the biradical can change strongly, but no additional unknown parameters appear. The spin of the nucleus and the gyromagnetic ratio of the nucleus change under the isotope substitution. As a result, the HFI constant of unpaired electrons with magnetic nuclei changes. But this change takes place in a perfectly known manner. Therefore, under the isotope substitution, changes in the spectrum can be predicted theoretically. This opens up the possibility of independent fitting of the experimental spectrum. This allowed us to fairly convincingly evaluate the relative content of biradicals in various conformations with different exchange integrals J. The study of the asymmetric biradical in which the radical centers have different nitrogen isotopes was especially important, since in symmetric biradicals, in the absence of conformational transitions, in principle, it is impossible to distinguish biradicals with $J = 0$ from monoradicals using EPR spectra.

The study of the temperature dependence of the EPR spectrum of biradicals made it possible to estimate rather convincingly that at room temperatures about 20% of nitroxide biradicals **B1, B2, B3** have a conformation with negligible in EPR experiments exchange integral, J=0, about 75% of those biradicals have $|J|$=4.4G, and the rest 5% of biradicals have $|J|$=11.2 G and $|J|$=57G in almost equal amounts.

For further applications of biradicals, it is of major importance that the asymmetric biradical **B2** have relatively weak exchange interaction, i.e., the exchange integral is much less than the nitrogen-induced HFI splitting of EPR lines. Due to this fact electron spins in these biradicals can be selectively excited by the microwave pulses. At the same time, the exchange interaction is strong enough to be able to create entangled states of two unpaired electrons of those biradicals. So, the biradicals **B2** may be of use in quantum computing and quantum informatics [11].

Acknowledgements Authors T. Kálai and K. Kish (Pécs University) gratefully acknowledge the support of the grant GINOP-2.3.2-15-2016-00049.

References

1. V.N. Parmon, A.I. Kokorin, G.M. Zhidomirov, Russ. J. Struct. Chem. **18**, 104 (1977)
2. E.G. Rozantsev, *Free Nitroxyl Radicals* (Plenum Press, New York, 1970)
3. L.B. Volodarsky (ed.), *Nitroxide. Synthesis, Properties, Applications*, 1st–2 edn. (CRC Press, Boca Raton, 1988)
4. R.I. Zhdanov (ed.), *Bioactive Spin Labels* (Springer, Berlin, 1992)
5. A. Rassat, Pure Appl. Chem. **62**, 223 (1990)
6. M.T. Lemaire, Pure Appl. Chem. **76**, 277 (2004)
7. M. Abe, Chem. Rev. **113**, 7011 (2013)
8. Yu.N. Molin, K.M. Salikhov, K.I. Zamaraev, *Spin Exchange* (Springer, Berlin, 1980)
9. B.D. Armstrong, S. Han, J. Chem. Phys. **127**, 1045081 (2007)
10. M.J. Prandolini, V.P. Denysenko, M. Gafurov, S. Lyubenova, B. Endeward, M. Bennati, T.E. Prisner, Appl. Magn. Reson. **34**, 399 (2008)
11. K. Sato, S. Nakazawa, R. Rahimi, T. Ise, S. Nishida, T. Yoshino, N. Mori, K. Toyota, D. Shiomi, Y. Yakiyama, Y. Morita, M. Kitagawa, K. Nakasuji, M. Nakahara, H. Hara, P. Carl, P. Höfer, T. Takui, J. Mater. Chem. **19**, 3739 (2009)
12. A.B. Shapiro, M.G. Goldfield, E.G. Rozantsev, Tetrahedron Lett. **14**, 2183 (1973)
13. V.V. Pavlikov, V.V. Muraviev, A.B. Shapiro, Izv. AN SSSR Ser. Khim **5**, 1200 (1980)
14. S. Torii, T. Hase, M. Kuroboshi, C. Amatore, A. Jutand, H. Kawafuchi, Tetrahedron Lett. **38**, 7391 (1997)
15. A.I. Kokorin, Appl. Magn. Reson. **26**, 253 (2004)
16. A.I. Kokorin, V.V. Pavlikov, A.B. Shapiro, Proc. Acad. Sci. Phys. Chem. **253**, 147 (1980)
17. A.B. Shapiro, V.N. Parmon, V.V. Pavlikov, V.I. Rubtsov, E.G. Rozantsev, Izv. AN SSSR Ser. Khim. **2**, 449 (1980)
18. A.I. Kokorin, V.A. Tran, K. Rasmussen, G. Grampp, Appl. Magn. Reson. **30**, 35 (2006)
19. V.A. Tran, A.I. Kokorin, G. Grampp, K. Rasmussen, Appl. Magn. Reson. **35**, 389 (2009)
20. A.I. Kokorin, E.N. Golubeva, B. Mladenova, V.A. Tran, T. Kálai, K. Hideg, G. Grampp, Appl. Magn. Reson. **44**, 1041 (2013)
21. S.Y. Umanskiy, E.N. Golubeva, B.N. Plakhutin, Russ. Chem. Bull. **62**, 1511 (2013)
22. A.I. Kokorin, O.I. Gromov, T. Kálai, K. Hideg, Appl. Magn. Reson. **47**, 1283 (2016)
23. A.I. Kokorin, R.B. Zaripov, O.I. Gromov, A.A. Sukhanov, T. Kálai, E. Lamperth, K. Hideg, Appl. Magn. Reson. **47**, 1057 (2016)
24. A.I. Kokorin, R.B. Zaripov, O.I. Gromov, K. Hideg, T. Kálai, Appl. Magn. Reson. **49**, 137 (2018)
25. L.A. Shundrin, I.A. Kirilyuk, I.A. Grigor'ev, Mendeleev Commun. **24**, 298 (2014)
26. T. Kálai, J. Jeko, Z. Berente, K. Hideg, Synthesis **38**, 439 (2006)
27. J.A. Riddick, W.B. Bunger, K.T. Sakano, *Techniques of Chemistry: Organic Solvents, Physical Chemistry and Methods of Purification*, 2nd edn. (Wiley, New York, 1986), p. 785
28. Ya.S. Lebedev, O.Ya. Grinberg, A.A. Dubinsky, O.G. Poluektov, in *Bioactive Spin Labels*, ed. by R.I. Zhdanov (Springer, Berlin, 1992), p. 227
29. A.M. Portis, Phys. Rev. **97**, 1071 (1953)